Earth Planets Space, **54**, 819–830, 2002

The 2000 Western Tottori Earthquake—Seismic activity revealed by the regional seismic networks—

Shiro Ohmi, Kunihiko Watanabe, Takuo Shibutani, Norio Hirano, and Setsuro Nakao

Disaster Prevention Research Institute, Kyoto University, Uji, Kyoto 611-0011, Japan

(Received September 12, 2001; Revised July 12, 2002; Accepted July 15, 2002)

On October 6, 2000, the 2000 Western Tottori Earthquake (Mjma 7.3) occurred in the western Tottori prefecture area, southwestern Japan. It initiated at a depth of 12 km at the bottom of the seismogenic zone, which was derived from aftershock distribution. The aftershocks extend over a 35 km length in a north-northwest direction. Spatial and temporal distribution of the aftershocks exhibits local characteristics in the fault region. The northern part consists of earthquake clusters while the southern part consists of a rather simple lineament of aftershocks, and the spreading and decaying rate of the aftershocks is slower in the northern part. This contrast is possibly due to the heterogeneity of the fault system and probably affected the rupture process of the mainshock. Two swarm sequences occurred in the surrounding region after the mainshock. One initiated 48 hours after the mainshock 25 km southwest of the main aftershock distribution. The other started 20 hours after the mainshock northeast of the mainshock on the southeast flank of Daisen volcano. These activities are probably induced seismicity due to stress changes in the focal region. Pre-seismic swarm activities occurred in the focal region from 1989 and deep low-frequency earthquakes were observed since 1999. It is important to understand the relationship between these possible precursory phenomena and the occurrence of the mainshock.

1. Introduction

On October 6, 2000, an Mj 7.3 earthquake shook western Tottori prefecture, Chugoku district, southwestern Japan. It was named the 2000 Western Tottori Earthquake by the Japan Meteorological Agency (JMA). Figure 1 shows a map of the Tottori prefecture and surrounding region and Fig. 2 is a map of seismicity in this area. Earthquakes from the catalogue of the Disaster Prevention Research Institute, Kyoto University (DPRI) from 1976 until the end of September 2000 are plotted in Fig. 2. In the Tottori area, a lineament of seismicity nearly parallel to the coast line is prominent in the central to eastern area and swarm activities are observed in the western area. The 2000 Western Tottori Earthquake is located in the western Tottori prefecture region where swarm activity had been observed. Figure 1 also shows the location and focal mechanism of the mainshock determined using seismic data of the regional seismic network for monitoring microearthquake activity. The mainshock initiated about 3 km north-northwest (NNW) of the Kamakura-Yama Nanpo fault at a depth of 12 km. This is an active fault with a designated activity level 3 by the Active Fault Research Group (1991). In this paper, we will describe the seismic activity and related phenomena of the 2000 Western Tottori Earthquake derived from the analyses of the seismic data from the regional seismic networks.

2. Relocation of Hypocenters

In the Chugoku district, southwestern Japan, a seismic network for monitoring microearthquakes has been operated by DPRI since the mid-1970's (e.g. Kishimoto *et al.*, 1978; Ohmi *et al.*, 1999). In the late-1990's particularly after the 1995 Southern Hyogo Earthquake (Kobe Earthquake), JMA and the National Research Institute for Earth Science and Disaster Prevention (NIED) established new high sensitivity seismic networks nationwide (e.g. Hi-net).

Seismograms recorded by these systems are read by seismic analysts at the Tottori Observatory of DPRI (Tottori Obs.) and JMA, so high quality hypocenter locations are expected when merging arrival time data from the two systems. Thus Ohmi (2002) conducted a hypocenter relocation using arrival time data from the two systems. Figure 3 shows seismic stations used for hypocenter relocation in Ohmi (2002). They consist of eight DPRI stations, five JMA stations and 15 Hi-net stations. Two stations out of eight DPRI stations are temporarily installed ones after the mainshock for monitoring aftershock activity.

In Ohmi (2002), they applied a method HYPOHO, which was developed by Hurukawa and Ohmi (1993). This is a simple method to determine hypocenters taking into account the lateral heterogeneity of the earth. In the HYPOHO method, we calculate hypocenters using station corrections as a function of hypocenter coordinates (x, y, z). The lateral heterogeneity is corrected by these station corrections. We assumed the station correction τ_j at the j-th station is represented as follows:

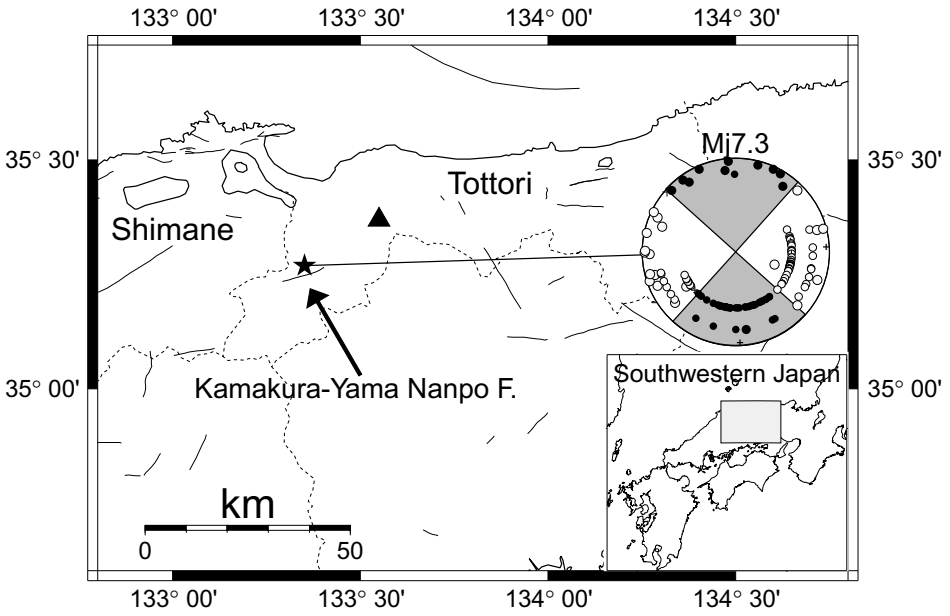

Fig. 1. Index map of Tottori prefecture and surrounding region. Dotted lines show the prefecture borders and thick lines represent the active faults. Daisen volcano, which is a Quaternary volcano, is denoted by a solid triangle. Epicenter of the 2000 Western Tottori Earthquake is shown by a star. Focal mechanism of the mainshock obtained from first motion of P-waves is also shown. Polarities of first motion are denoted by solid (up) and open (down) circles.

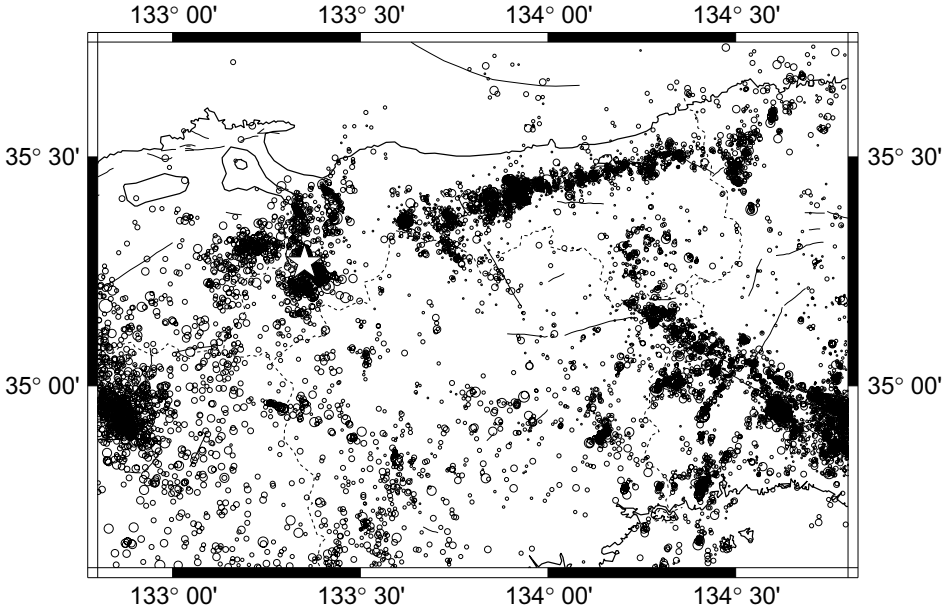

Fig. 2. Seismicity in the Tottori and surrounding region. Earthquakes from 1976 until the end of September 2000 from the catalogue of DPRI are plotted. Epicenter of the 2000 Western Tottori Earthquake is shown by a star.

$$\begin{aligned}\tau_j &= C_{0j} + C_{1j}x + C_{2j}y + C_{3j}z \\ &\quad + C_{4j}xy + C_{5j}yz + C_{6j}zx \\ &\quad + C_{7j}x^2 + C_{8j}y^2 + C_{9j}z^2 \\ &= \sum_{k=0}^{9} C_{kj} H_k(x, y, z)\end{aligned}$$

where $C_{kj}(k = 0, 9)$ are constant for the j-th station. Using initial hypocenter locations in the target region, we can evaluate the station correction coefficients C_k for each station using a least squares scheme. Using station correction coefficients C_{kj}, we again relocate the hypocenter of each earthquake with a set of station corrections calculated using C_{kj} and the initial hypocenter coordinate of the earthquake.

Figure 4 shows the travel time residuals of the preliminary hypocenters by the Tottori Obs. and the relocated hypocenters by Ohmi (2002). It is recognized that relocated hypocenters have less travel time residuals. In this report, we use these relocated hypocenters.

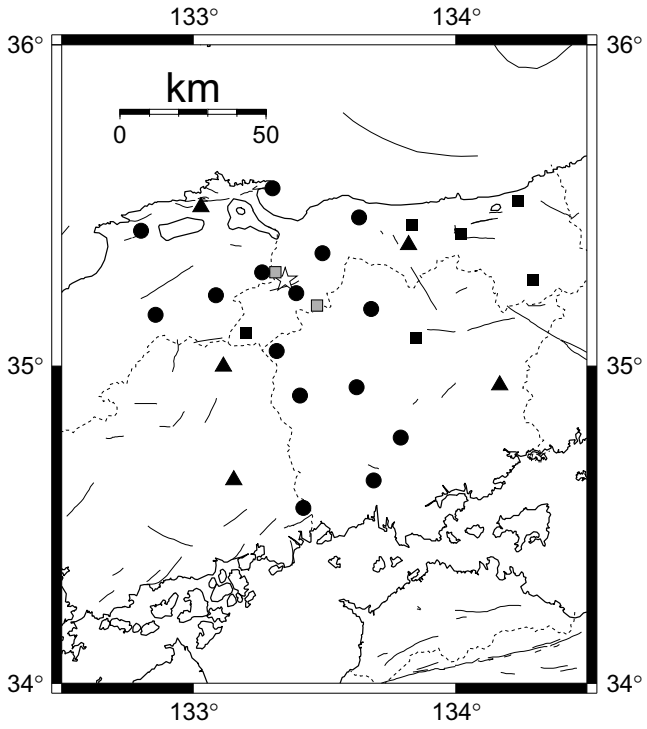

Fig. 3. 28 seismic stations used for locating hypocenters. Eight DPRI stations (squares), five JMA stations (triangles) and 15 Hi-net stations (circles). Gray squares are temporarily installed stations by DPRI. Epicenter of the mainshock is shown by a star.

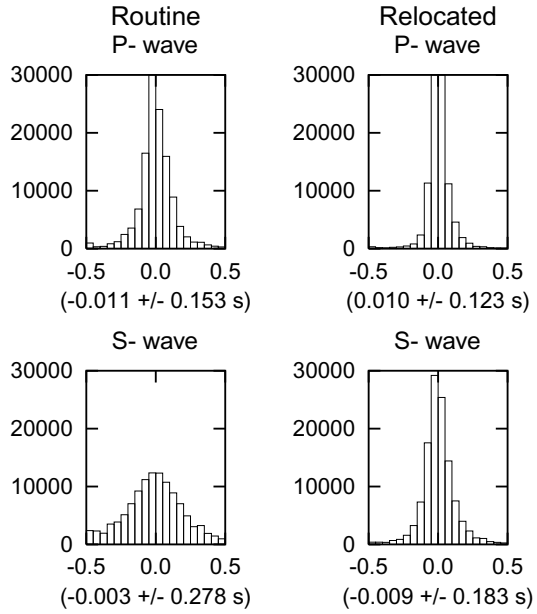

Fig. 4. Histograms of travel time residuals. The horizontal axis is in seconds and the vertical axis represents the number of arrival time data. The averages and the standard deviations of the travel time residuals are also shown. On the left are the residuals for earthquakes located in the routinely operation in Tottori Obs. On the right are the results for the relocated earthquakes.

3. Mainshock and Aftershock Activity

3.1 Mainshock

Hypocenter of the 2000 Western Tottori Earthquake relocated is as follows: origin time = 13:30:18.1 JST on October 6, 2000; latitude = 35.270°N; longitude = 133.352°E; focal depth = 12.2 km. Hypocenter and focal mechanism solution are shown in Fig. 1. In this analysis, we used arrival time data from stations within 130 km for the hypocenter determination, and polarity data of the initial P-wave onset from stations within 300 km from the epicenter. Strike, dip, and rake angles of two nodal planes are (132°, 90°, 0°) and (222°, 90°, −180°), respectively. From the trend of the aftershocks, the plane with strike of 132° is probably the fault plane.

When comparing the focal mechanism solution from first motion analysis (Fig. 1) with the precise determined aftershock distribution (Fig. 6(b)), it is recognized that the trend of aftershocks does not coincide with the nodal plane of N132°E (N48°W). Aftershock distribution of only about 3 km long to the south and 4 km long to the north of the epicenter of the mainshock are aligned in the trend of the nodal plane. Source process analysis of the mainshock (e.g. Sekiguchi *et al.*, 2001; Iwata and Sekiguchi, 2002) indicates the existence of large slip (>2 m) at 7 km long to the south of the epicenter. Focal mechanism solution obtained from the first motion analysis is affected by the geometry of the ruptured area at the mainshock. We suppose that the nodal plane of N132°E obtained is constrained by the large slip area of the mainshock around the epicenter, whose direction is shown by the alignment of aftershock distribution near the epicenter.

3.2 Aftershocks immediately after the mainshock

Figure 5 shows snapshots of the epicenter distributions immediate after the mainshock. These are epicenter distributions for an hour after the mainshock, and the succeeding 2 hours, 4 hours, 8 hours, 16 hours and 32 hours. During the several hours after the mainshock, the NNW part of the hypocenter of the mainshock (roughly northern part of the Kamakura-Yama Nanpo fault) is more active than the south-southeast (SSE) part. Aftershock activity in the SSE part quickly spread throughout the whole area within several hours, while in the NNW area it took about one day to spread out.

3.3 Aftershock activity

Figures 6 and 7 show the relocated aftershock distributions and space-time plots during the period between October 2000 and March 2001. Figure 8 shows the change in number of aftershocks with time.

Figure 6(a) shows the whole relocated aftershocks while Fig. 6(b) shows the precisely relocated aftershocks until the end of March 2001. On Fig. 6(b), relocated earthquakes with following criteria are plotted; (1) Number of P-picks ≥20, (2) Number of S-picks ≥20, (3) RMS of P travel time residuals ≤0.1 s, and (4) RMS of S travel time residuals ≤0.3 s. Figure 6(b) demonstrates that the hypocenter of the mainshock is located at the lower boundary of the aftershock distribution, which indicates the rupture initiated at the bottom of the seismogenic zone. This tendency was reported for some other large crustal earthquakes. For example, the 1995 Southern Hyogo Earthquake (Mj 7.2) (e.g. Nakamura and Ando, 1996) also initiated from the bottom of the seismogenic zone. Our observation is probably another example of this trend.

It is also clear that aftershock activity exhibits different features between the NNW and SSE parts of the aftershock

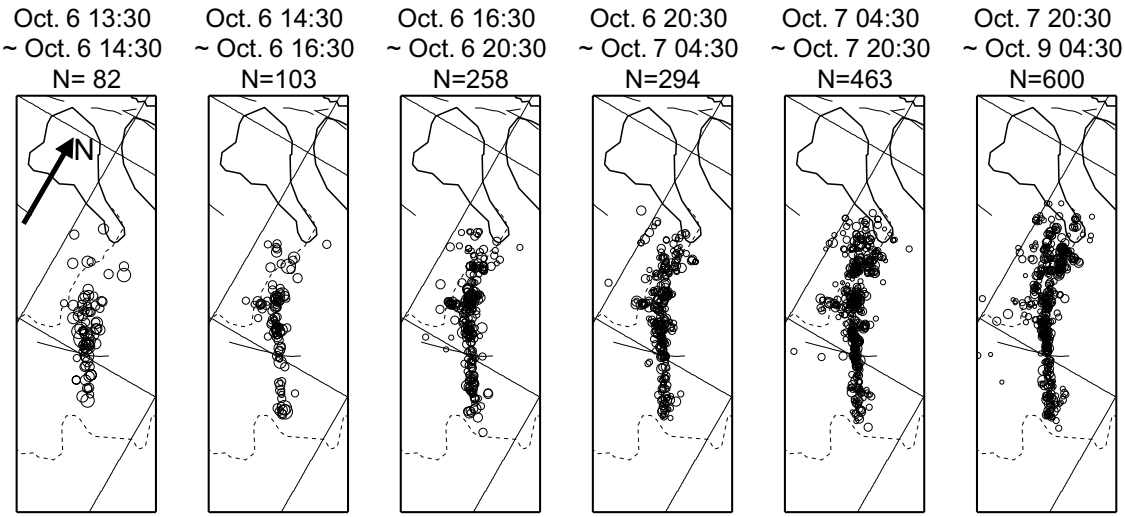

Fig. 5. Snapshots of aftershocks immediately after the mainshock. They are epicenter distributions within an hour after the mainshock, and the succeeding 2 hours, 4 hours, 8 hours, 16 hours and 32 hours, respectively.

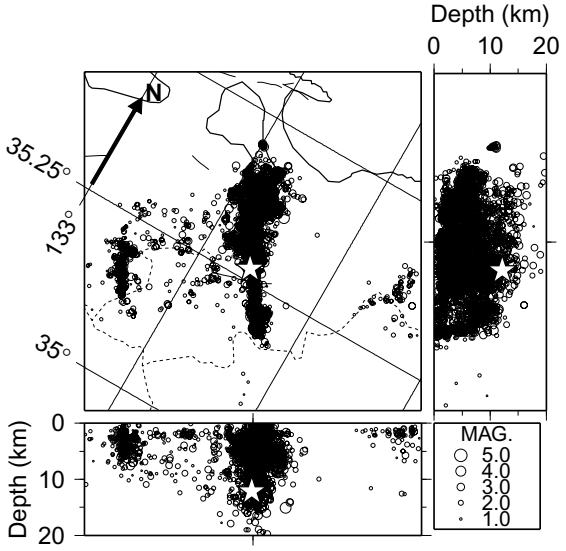

Fig. 6(a). Relocated aftershock distribution in western Tottori prefecture area from October 2000 to March 2001. More than 6500 earthquakes are plotted. Mainshock is denoted by a star.

distribution. In the SSE part, aftershocks aligns in a thin, nearly vertical plane with a thickness of 2–3 km, while in the NNW part there are some clusters aligning in a north-northwest direction (Fig. 6(b)). The area with less seismicity in the SSE part seems to correspond to the area with large slip during the mainshock (e.g. Sekiguchi *et al.*, 2001; Iwata and Sekiguchi, 2002).

The spreading rate of the aftershocks is faster in the SSE part of the mainshock (Fig. 5). On the other hand, Fig. 7(a) demonstrates the decay of aftershock activity is also faster in the SSE part. In other words, in the NNW part of the mainshock, aftershock activity slowly spread throughout the area and attenuates slowly, and vise versa. The distribution of aftershocks (Fig. 6(b)) indicate that the NNW part of the fault system is more complex than the SSE part, and thus the NNW part possibly took longer time to release the stress with gradually breaking the NNW part of the fault system.

3.4 Aftershocks in the surrounding area

Enhancement of seismic activity was observed in the surrounding area after the mainshock. Figure 6(a) shows two other swarms other than main aftershock distribution.

On October 8, 2000 at 20:51 JST, the largest aftershock (Mj 5.0) occurred in the northern part of the main aftershock distribution (Event B on Fig. 9). Another large event (Mj 5.5) took place on October 8, 2000 at 13:17 JST, which is 48 hours after the mainshock followed by aftershock activity (Event C on Fig. 9). It is located about 25 km southwest of the main aftershock distribution. The alignment of this distribution is nearly parallel to that of the main aftershocks. Another swarm was observed on the southeast flank of Daisen volcano starting 20 hours after the mainshock. Space-time plot of these activities are shown in Fig. 7(b).

These surrounding swarms are not considered as aftershocks in the strict sense since they are not on the fault plane of the mainshock. However, they are probably examples of off-fault aftershock activity due to the stress change in the region caused by the mainshock. Similar induced activity was also observed after the 1995 Southern Hyogo Earthquake. Soon after the mainshock, seismic activity in the Kinki area increased (e.g. Katao, 1995).

4. Foreshock and Deep Low-Frequency Earthquakes

A foreshock of M = 1.7 was observed 12 hours prior to the mainshock near the hypocenter of the mainshock. The hypocenter located using a master event method (e.g. Ito and Kuroiso, 1979) with mainshock is about 3 km apart from the hypocenter of the mainshock. From the trend of the aftershocks, this foreshock probably occurred on the fault plane of the mainshock. Figure 10 shows the hypocenter location of the foreshock together with that of the mainshock.

In the focal region of the 2000 Western Tottori Earthquake, swarm activities were observed in 1989, 1990 and 1997 with Mj = 5.1–5.4 earthquakes. These swarms are also recognized as 'long term foreshock activity' (e.g. Umeda *et al.*,

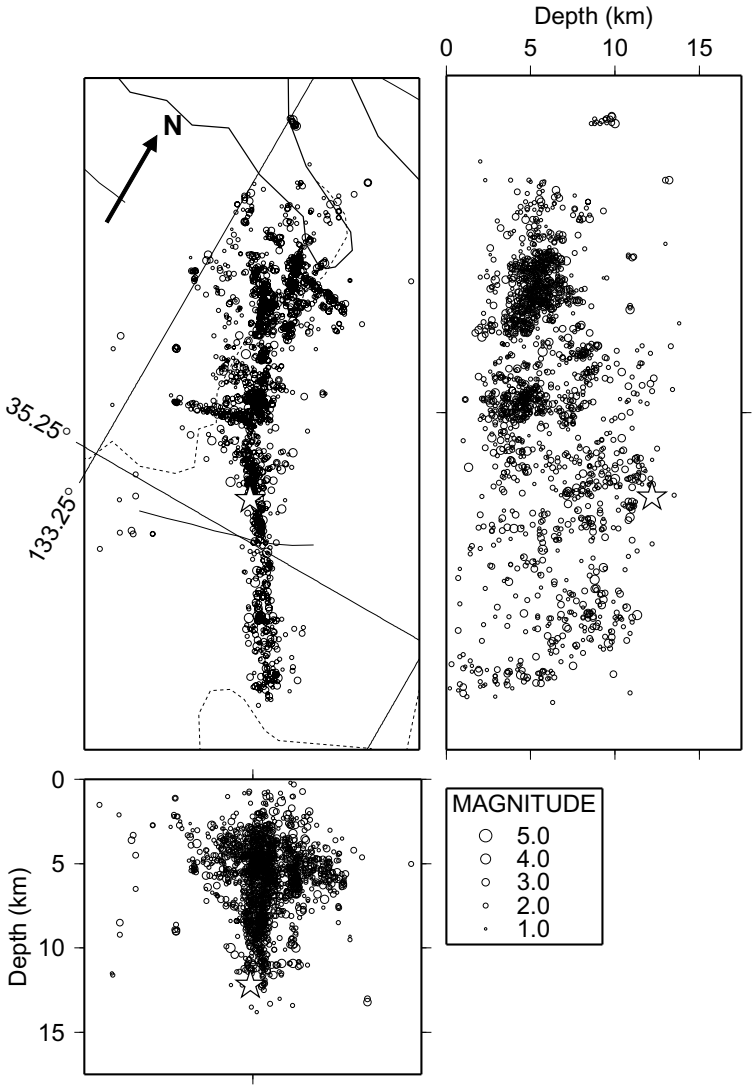

Fig. 6(b). Precisely relocated aftershocks from October 2000 to March 2001. About 1900 earthquakes are plotted. Mainshock is denoted by a star.

2001).

According to the JMA hypocenter catalogue, 4 deep low-frequency earthquakes (DLF) were observed before the mainshock (Ohmi and Obara, 2002). They are located about 8 km west of the mainshock at around 30 km depth. Three of them occurred in June and July 1999 and one in June 2000. DLF activity is also observed after the mainshock and during the one year from October 2000 to September 2001, more than 50 DLF events were observed. Figure 11(a) shows the hypocenters of the DLF events based on the JMA hypocenter catalogue while Fig. 11(b) is a space-time plot of DLF events together with shallow seismic activity from January 1997 until December 2001. Ohmi and Obara (2002) examined the continuous record of station TRT (Fig. 11(a)) and found another DLF event that took place on October 6, 2000 at 04:27 JST, about nine hours prior to the mainshock. The hypocenter is located near the region where the four other DLF events occurred.

Observed features in the waveform of these DLF events described by Ohmi and Obara (2002) are as follows; (1) Predominant frequency is 2 Hz–4 Hz (Fig. 12), however they are not monochromatic events, (2) Both P- and S-waves are observed however S-waves have larger amplitudes, and (3) The onset of the P-wave has a high-frequency component.

Figure 12 shows the spectra of two DLF's observed at stations TRT and some other stations near the epicenter. Figure 13 represents the spectral structure of ordinary earthquakes whose ray paths sample the source region of the DLF events, which remain high-frequency components. Therefore we conclude that the low-frequency nature of the DLF is originated from the source.

The durations of these events are one minute or longer, and in some cases they exhibit durations of several minutes. A DLF event on June 2000 had a duration of more than five minutes and continuous occurrence of DLF events were observed in a tremor-like waveform. Figure 14 shows the vertical components of 6 DLF events observed at station TRT.

Figure 15 shows the magnitude-frequency diagram of ordinary earthquakes and DLF events. Magnitudes of these DLF events ranges from 1.4 to 2.2, which indicates the differences of source mechanisms between shallow earthquakes and DLF events.

Ohmi and Obara (2002) analyzed the focal mechanism of

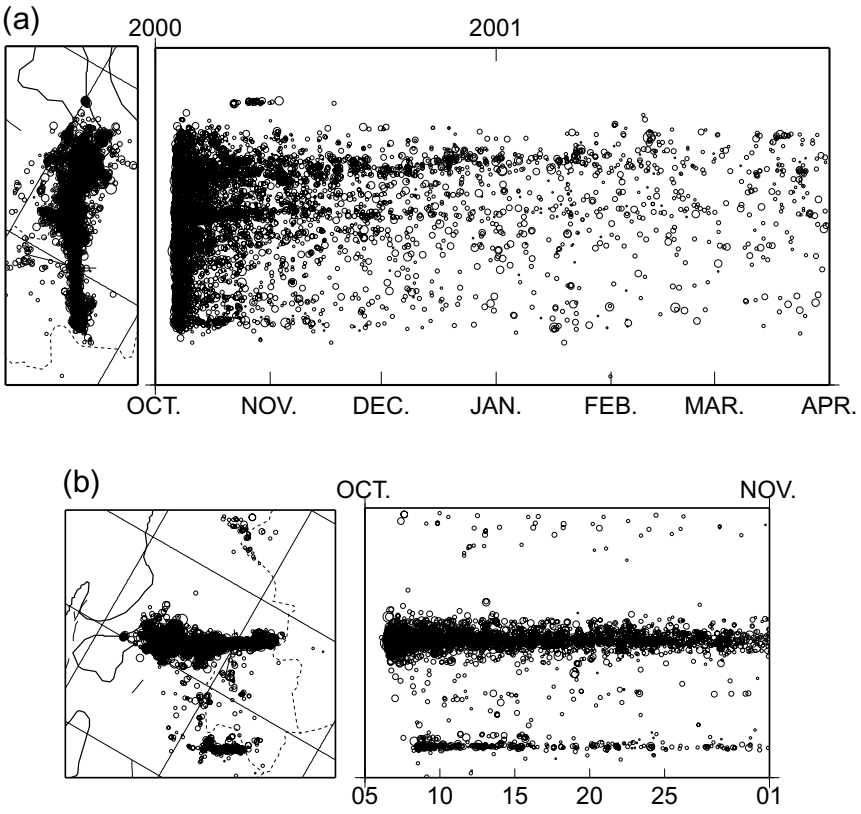

Fig. 7. Space-time plots of the aftershock distribution in western Tottori prefecture area. (a) Epicenters projected onto the N30°W section. (October 1, 2000–March 31, 2001). (b) Epicenters projected onto the N60°E section. (October 5, 2000–October 31, 2000).

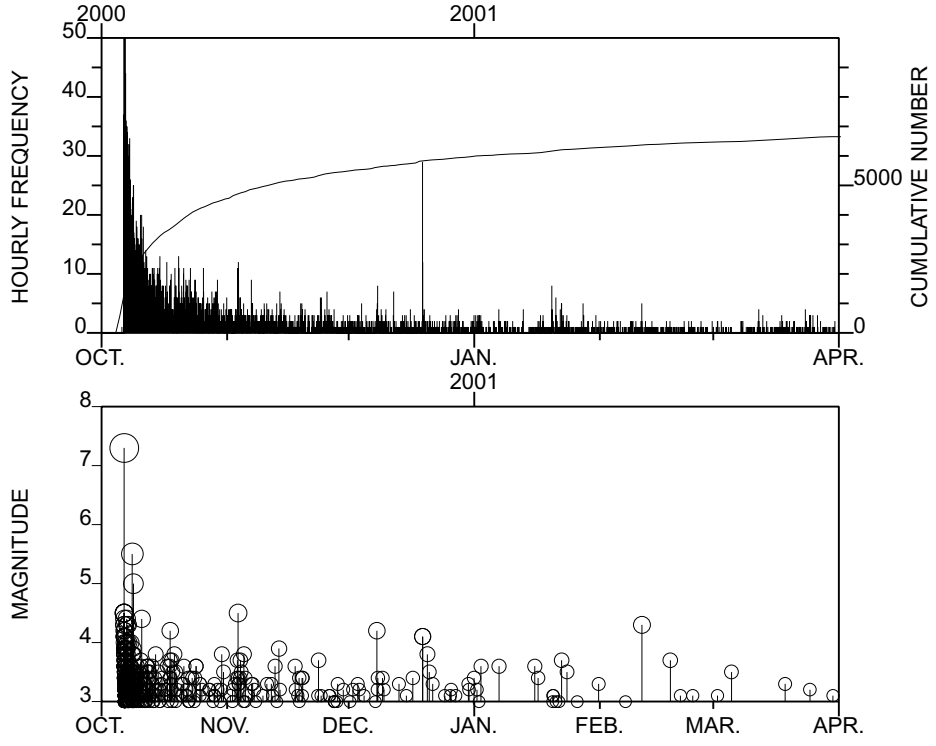

Fig. 8. Change of aftershock activity with time. Hourly frequency (upper, histogram), cumulative number (upper, line), and magnitude-time diagram (lower) of the aftershocks shown in Fig. 6(a). The JMA hypocenter catalogue is used to make the magnitude-time diagram.

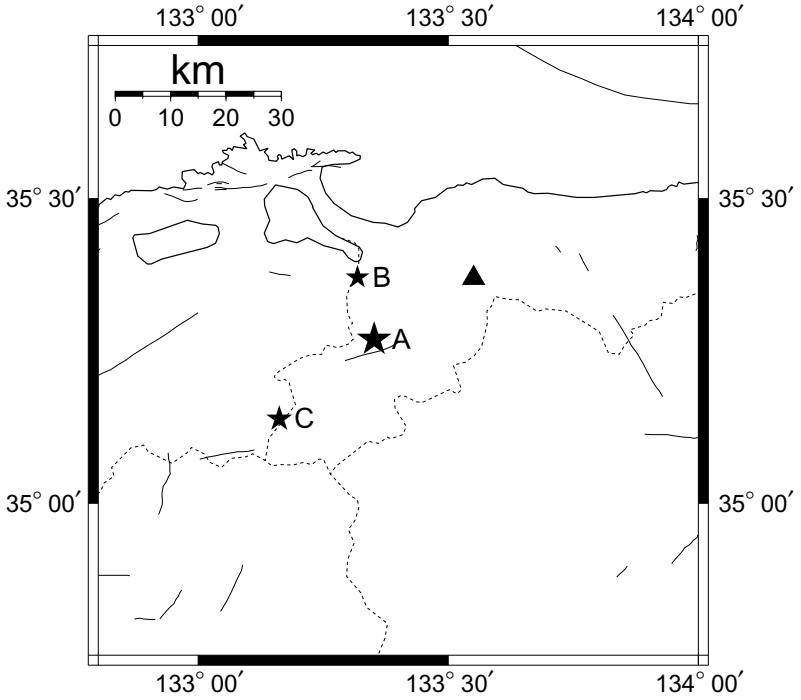

Fig. 9. Location of three largest earthquakes in the focal region. Event A shows the mainshock and B and C denote the largest aftershocks on October 8, 2000. For other symbols, see Fig. 1.

the DLF event took place on October 6, 2000 using the amplitude ratio of the P-wave to the S-wave and the polarization of the S-waves. They concluded that the single-force type source model is more preferable than an ordinary double-couple source model, which indicates the transport of fluid. Ukawa and Ohtake (1987) proposed a model of DLF event, that consists of two fluid reservoirs connected by a conduit. It is outlined as follows; Usually the conduit is closed. When the pressure difference between the two reservoirs exceeds the threshold, the conduit is broken and high frequency seismic wave is radiated at this stage. After opening the conduit, fluid is transported in the conduit and low-frequency waves are radiated. Observed DLF events have low-frequency wave train with a high frequency component at the beginning, thus this is one possible model that explains the nature of the observed DLF events.

In previous studies, DLF events are mostly observed near active volcanoes or the volcanic front and attributed to magmatic activity (e.g. Hasegawa and Yamamoto, 1994; Ukawa and Obara, 1993). However there are no active volcanoes in the western Tottori region. Recent studies (e.g. Hasegawa *et al.*, 2001) indicate the existence of fluid such as water beneath active faults that causes the decrease of shear strength of the fault. DLF events observed in western Tottori region are probably another piece of evidence that indicates the existence of fluids beneath an active fault zone. It is important to understand the nature of DLF events as a sign of the behavior of fluids in the focal region that might trigger the rupture of the fault.

5. Discussion and Conclusion

In this paper we described the seismic activity and related phenomena of the 2000 Western Tottori Earthquake that occurred at 13:30:18.2 JST on October 6, 2000. The mainshock initiated at about 3 km north-northwest to the Kamakura-Yama Nanpo fault at a depth of 12 km. The main aftershock zone extends for 35 km in a north-northwest direction. The precisely relocated aftershock distribution exhibits differences in seismic activity between NNW and SSE parts of the hypocenter of the mainshock; the NNW part consists of some earthquake clusters while SSE part consists of rather simple lineament of aftershocks. The patterns of spreading and decaying of the aftershocks are also different between

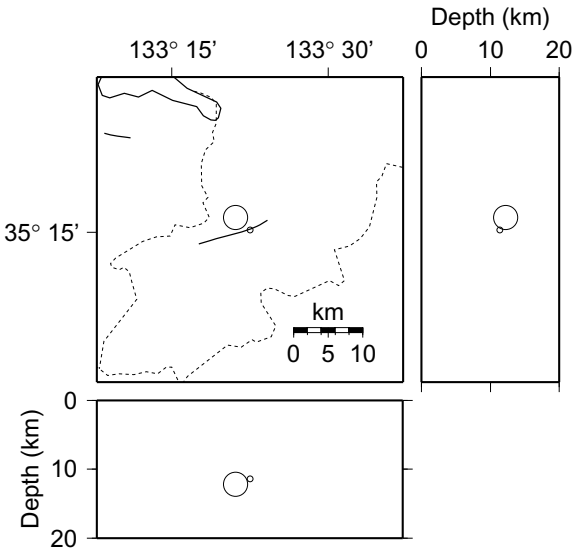

Fig. 10. Foreshock that occurred 12 hours prior to the mainshock, which is located by using the master event method with the mainshock. Large and small circles denote the mainshock and the foreshock, respectively.

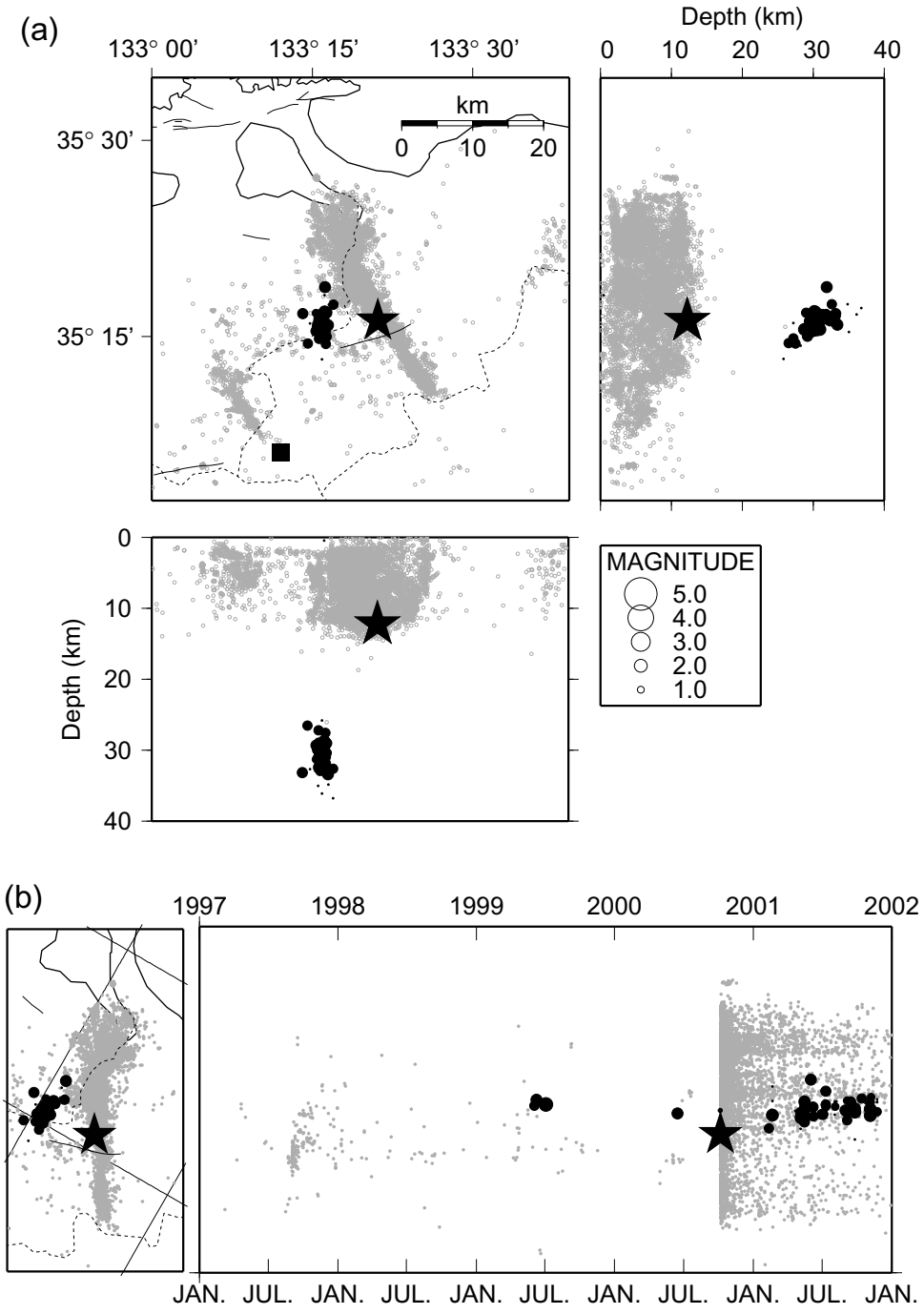

Fig. 11. Location of the deep low-frequency (DLF) earthquakes in the focal region of the 2000 Western Tottori Earthquake. They are located about 30 km depth and 8 km west of the hypocenter of the mainshock. Solid circles represent the hypocenters of the DLF earthquakes. Solid star denotes the mainshock and gray circles shows the shallow activity from 1997 to 2001. DLF earthquakes are from the catalogue of JMA while shallow earthquakes are from the catalogue of the Tottori Obs. (a) Distribution of hypocenters of DLF events. Solid square denotes the station TRT. (b) Space-time plot of the DLF events from 1997 until the end of 2001.

the NNW and SSE part. Aftershocks spread slowly and gradually decayed in the NNW part. They indicate the existence of the heterogeneity of the fault system; complex fault system is suggested in the NNW part and it possibly affected the rupture process of the fault during the mainshock.

Two swarm activities initiated in the surrounding region after the mainshock. One occurred 48 hours after the mainshock 25 km southwest of the main aftershock distribution. The other occurred 20 hours after the mainshock about 25 km northeast of the mainshock on the southeast flank of the Daisen volcano. These two activities are probably induced seismicity due to stress changes in the focal region.

Precursory swarms occurred in the focal region starting in 1989 and deep low-frequency earthquakes were observed since 1999. A foreshock ($M = 1.7$) was observed 12 hours prior to the mainshock, 3 km from the mainshock hypocenter.

The 2000 Western Tottori Earthquake (WT eq) is a large scale ($M > 7.0$) shallow inland earthquake in southwestern Japan. There is another example of large inland earthquakes

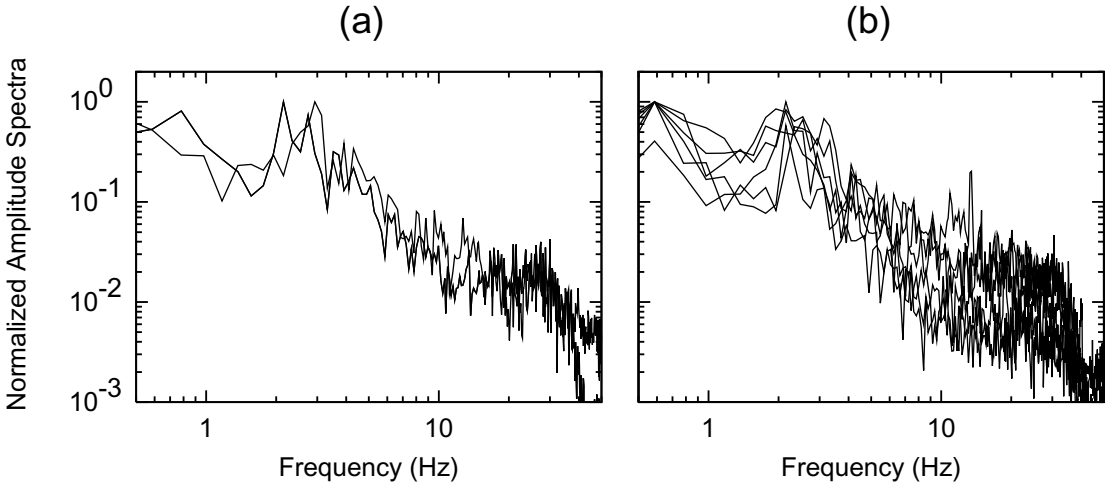

Fig. 12. Velocity spectra of DLF's. Normalized velocity spectra of a DLF occurred on October 6, 2000 (a) and that occurred on February 11, 2001 (b) are shown. High-pass filtered ($f_c = 0.2$ Hz) waveform of the vertical component observed at station TRT and some other nearby stations are used.

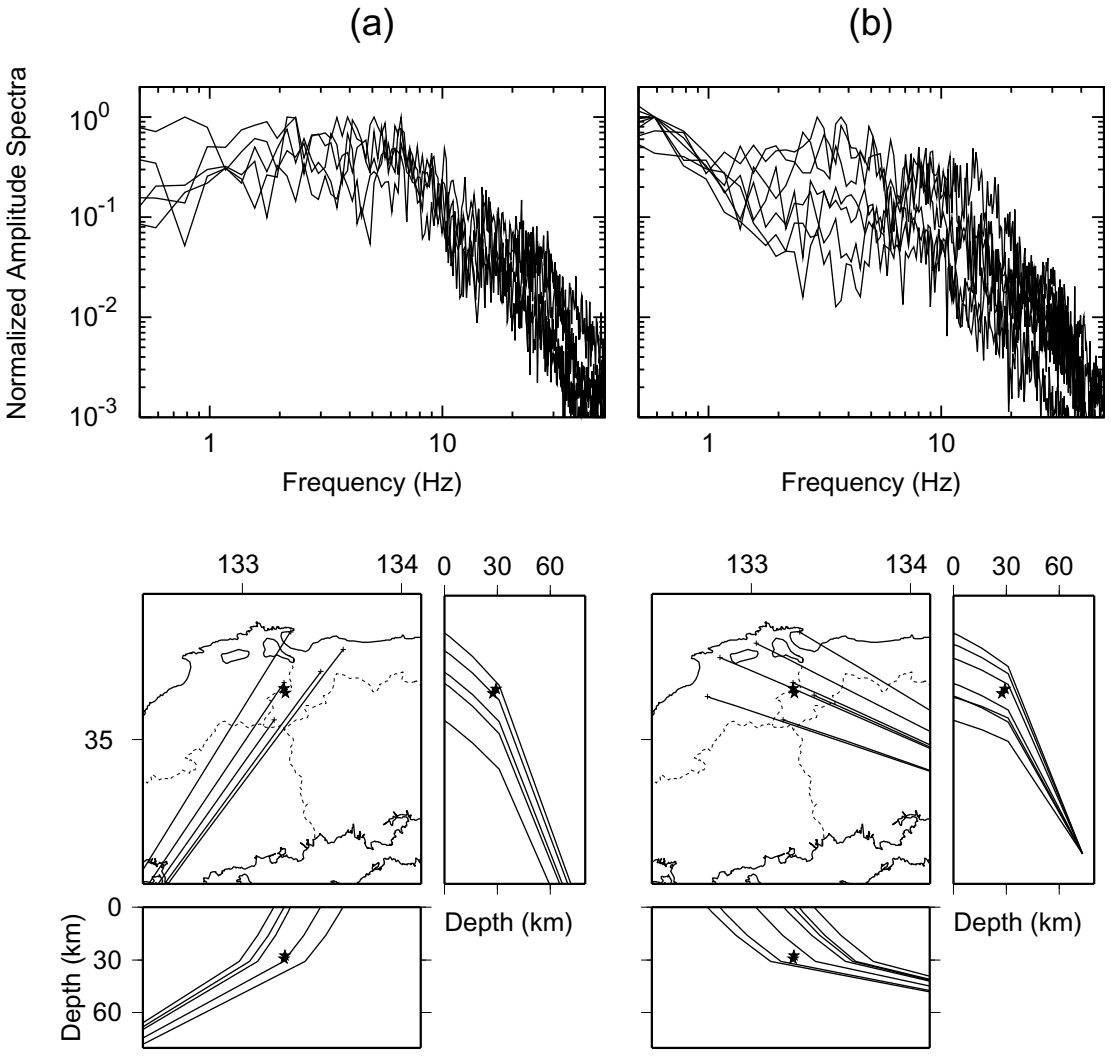

Fig. 13. Velocity spectra of two ordinary earthquakes. The ray paths of these earthquakes sample the source region of the DLF events. Figure 13(a) (left) shows the spectrum of an M3.7 event whose depth is 127 km, while Fig. 13(b) (right) shows that of an M3.2 event whose depth is 73 km. Upper plates show the spectra while lower plates represent the corresponding ray paths.

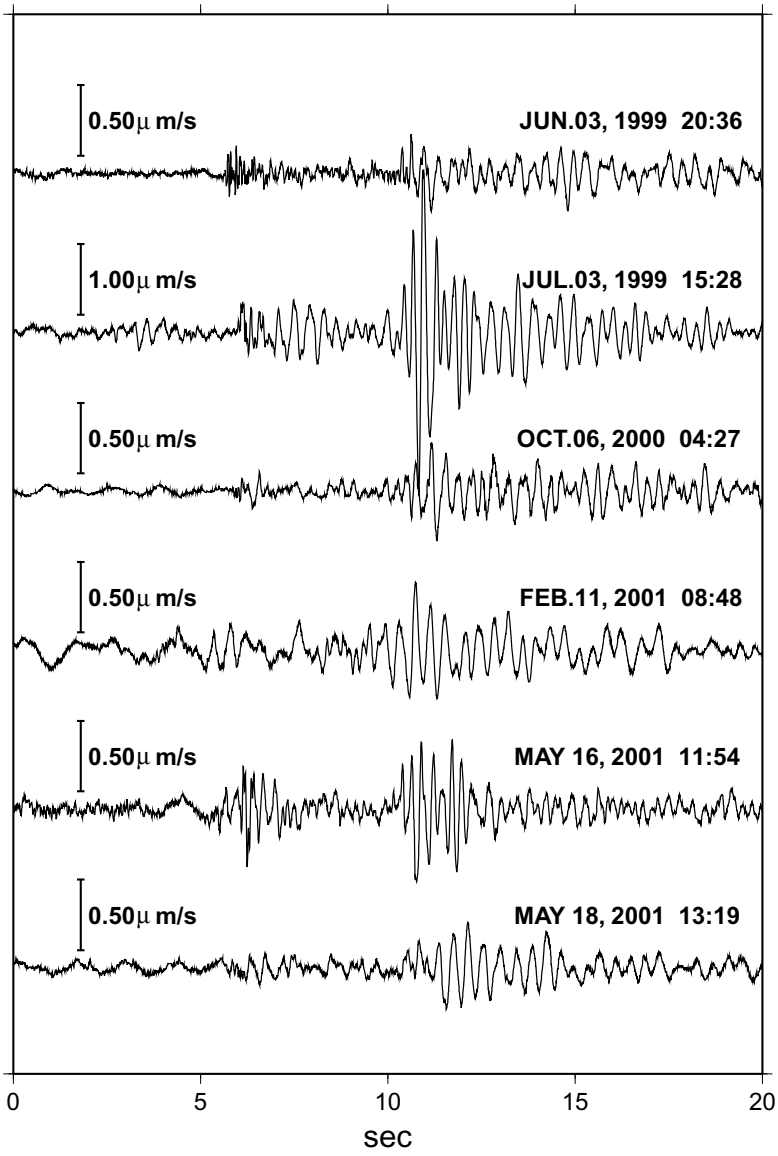

Fig. 14. Waveforms (vertical components) of the DLF earthquakes observed at station TRT. Top three traces show events that occurred before the mainshock while bottom three occurred after the mainshock.

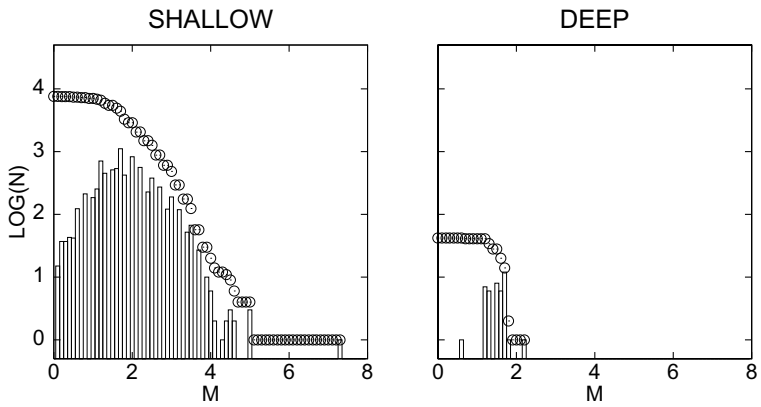

Fig. 15. Magnitude-frequency diagram of the shallow earthquakes in the Western Tottori region (left) and that of the DLF earthquakes beneath the focal region of the Western Tottori Earthquake (right).

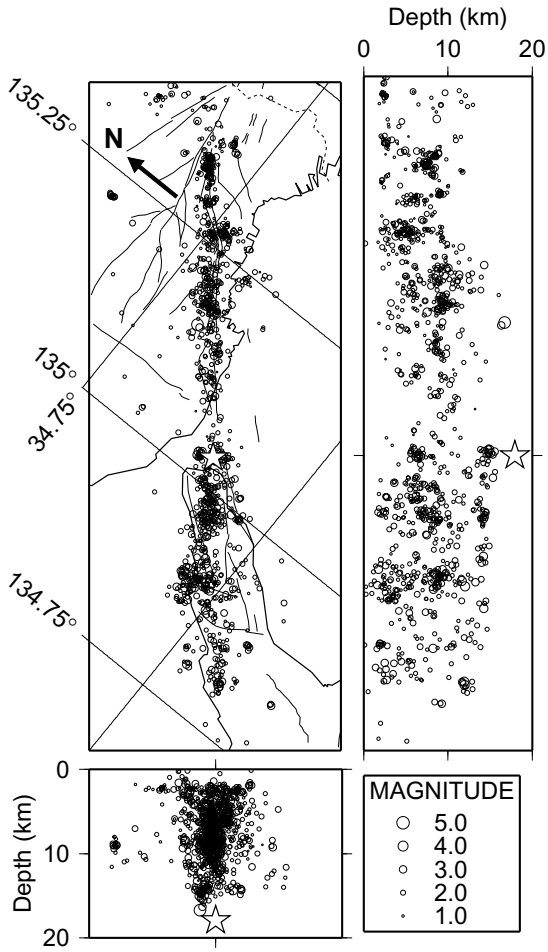

Fig. 16. Aftershock distribution of the 1995 Southern Hyogo Earthquake from January 27 to February 28, 1995. Mainshock located by the JMA is denoted by a star.

in southwestern Japan, which is the 1995 Southern Hyogo Earthquake (Mj 7.2). Finally, we will compare the characteristics of these two earthquakes from the observed seismic activity. On January 17, 1995, the 1995 Southern Hyogo Earthquake (SH eq) shooked the Kinki district, southwestern Japan and caused serious damage (e.g. Irikura and Ando, 1996). Figure 16 shows the aftershock distribution of the SH eq relocated by Ohmi (1995). The aftershock zone of the SH eq strikes N51°E and is about 60 km wide and 15 km deep (Nakamura and Ando, 1996). The mainshock initiated at the middest of the fault at the depth of 17.9 km (JMA), which is the base of the seismogenic zone. In the case of WT eq, the size of the aftershock region is 35 km wide and 15 km deep, and the rupture of the mainshock also started from the bottom of the aftershock region.

In the case of the SH eq, there is a clear inactive area in the aftershock zone near the hypocenter of the mainshock (Hirata *et al.*, 1996). On the other hand, in the case of WT eq, the area with less aftershock activity in the SSE part corresponds to the area with large slip during the mainshock. In both cases, fault areas that released the stress at the mainshock have less aftershock seismicity.

Heterogeneity of the fault system is also observed in both cases. In the case of the SH eq, at least seven clusters of aftershocks are observed, some of which distribute perpendicular to the mainshock fault strike (Hirata *et al.*, 1996).

There were 'long term foreshock activities' with earthquakes of $M > 5$ in the focal region of the WT eq. (e.g. Umeda *et al.*, 2001). On the contrary, there are no precursory seismic activity before the SH eq but four foreshocks eleven hours prior to the mainshock (Katao and Iio, 1995). In the focal region of the SH eq, seismic quiescence of 30 years was observed until 1995 (Mogi, 1995).

Although the size and characteristics of the two earthquakes are similar, appearance of the precursory phenomena is much different. It is significant issue to clarify the relationship between these precursory phenomena and the occurrence of large-scale inland earthquakes.

Acknowledgments. We are grateful to the National Research Institute for Earth Science and Disaster Prevention for providing us the Hi-net waveform data. We also thank the Japan Meteorological Agency for allowing us to use their waveform data, arrival time data, and Preliminary Determined Earthquake catalogue. Makoto Koizumi, Satoru Fujihara, and Yousuke Fujisawa helped with installation of temporal seismic stations. Haruko Takeuchi, Aiko Nakao, Sachie Miwa, Fumiaki Takeuchi, Azusa Shito, Kim Ai and Bogdan Enescu helped with reading seismograms. Two anonymous reviewers contributed helpful suggestions that improved the manuscript. The General Mapping Tool (Wessel and Smith, 1998) was used for drawing figures.

References

Active Fault Research Group, Active Faults in Japan (New edition), Tokyo Univ. Press, 437 pp., 1991.

Hasegawa, A. and A. Yamamoto, Deep, low-frequency microearthquakes in or around seismic low-velocity zones beneath active volcanoes in northeastern Japan, *Tectonophys.*, **233**, 233–252, 1994.

Hasegawa, A., N. Umino, and S. Hori, Seismic activity and heterogeneity of the crust in the Nagamachi-Rifu fault zone, *Monthly Chikyu*, **263**, 313–320, 2001.

Hirata, N., S. Ohmi, S. Sakai, K. Katsumata, S. Matsumoto, T. Takanami, A. Yamamoto, T. Iidaka, T. Urabe, M. Sekine, T. Ooida, F. Yamazaki, H. Katao, Y. Umeda, M. Nakamura, N. Seto, T. Matsushima, H. Shimizu, and Japanese University Group of the Urgent Joint Observation for the 1995 Hyogo-ken Nanbu Earthquake, Urgent joint observation of aftershocks of the 1995 Hyogo-ken Nanbu earthquake, *J. Phys. Earth*, **44**, 317–328, 1996.

Hurukawa, N. and S. Ohmi, A hypocenter-determination method using station corrections as a function of hypocenter coordinates, *J. Seismol. Soc. Jpn., Ser. 2*, **46**, 285–295, 1993.

Irikura, K. and M. Ando, Learning from the 1995 Hyogo-ken Nanbu Earthquake, *J. Phys. Earth*, **44**, i–v, 1996.

Ito, K. and A. Kuroiso, Detailed spatial distributions of foreshock and aftershock activities of small earthquakes, *J. Seismol. Soc. Jpn., Ser. 2*, **32**, 317–327, 1979.

Iwata, T. and H. Sekiguchi, Source model of the 2000 Tottori-ken Seibu earthquake and near-source strong ground motion, Submitted to 11th Japan Earthq. Eng. Symposium, 2002.

Katao, H., Activation of seismicity in the northern Kinki district, Reports of the Coordinating Committee for Earthquake Prediction, 54, 517–521, 1995.

Katao, H. and Y. Iio, Abnormal initial rise of the foreshock of the 1995 Southern Hyogo Prefecture earthquake, Reports of the Coordinating Committee for Earthquake Prediction, 54, 620–623, 1995.

Kishimoto, Y., K. Oike, K. Watanabe, T. Tsukuda, N. Hirano, and S. Nakao, On the telemeter observation system of the Tottori and the Hokuriku micro-earthquake observatory, *J. Seismol. Soc. Jpn., Ser. 2*, **31**, 265–274, 1978.

Mogi, K., Seismic activity before and after the 1995 Hyogoken-Nanbu Earthquake, Reports of the Coordinating Committee for Earthquake Prediction, 54, 557–567, 1995.

Nakamura, M. and M. Ando, Aftershock distribution of the January 17, 1995 Hyogo-ken Nanbu Earthquake determined by the JHD method, *J.*

Phys. Earth, **44**, 329–335, 1996.
Ohmi, S., Data processing of the urgent joint observation of aftershocks of the 1995 Hyogo-ken Nanbu earthquake, Programme and abstracts, The seismological society of Japan, No. 2, A39, 1995.
Ohmi, S., Aftershock distribution of the 2000 Western Tottori Earthquake by use of the station corrections as a function of hypocenter coordinates, *J. Seismol. Soc. Jpn., Ser. 2*, **54**, 575–580, 2002.
Ohmi, S. and K. Obara, Deep Low-Frequency Earthquakes beneath the Focal Region of the Mw 6.7 2000 Western Tottori Earthquake, *Geophys. Res. Lett.*, 2002 (in press).
Ohmi, S., K. Watanabe, N. Hirano, A. Nakagawa, F. Takeuchi, H. Katao, H. Takeuchi, T. Asada, M. Koizumi, K. Ito, H. Wada, T. Shibutani, S. Nakao, K. Matsumura, T. Konomi, K. Kondo, and H. Watanabe, SATARN system, a unified microseismic observation network in D.P.R.I. Kyoto University, Annuals of Disas. Prev. Res. Inst., Kyoto Univ., No. 42 B-1, 45–60, 1999.
Sekiguchi, H., T. Iwata, Y. Sugiyama, Y. Fusejima, and H. Horikawa, Faulting process and condition for its occurrence of 2000 Tottori-ken Seibu Earthquake, Abstracts, 2001 Japan Earth and Planetary Science Joint Meeting, S3-006, 2001.
Ukawa, M. and K. Obara, Low frequency earthquakes around Moho beneath the volcanic front in the Kanto district, central Japan, *Bull. Volcanol. Soc. Jpn.*, **38**, 187–197, 1993.
Ukawa, M. and M. Ohtake, A monochromatic earthquake suggesting deep-seated magmatic activity beneath the Izu-Ooshima volcano, Japan, *J. Geophys. Res.*, **92**, 12649–12663, 1987.
Umeda, Y., K. Matsumura, T. Shibutani, S. Ohmi, and H. Katao, The 2000 Western Tottori Earthquake—precursory swarm earthquake, main shock and aftershock—, *J. Natural Disaster Science*, **19-4**, 501–512, 2001.
Wessel, P. and W. H. F. Smith, New, improved version of the Generic Mapping Tools released, *EOS Trans. AGU*, **79**, 579, 1998.

S. Ohmi (e-mail: ohmi@rcep.dpri.kyoto-u.ac.jp), K. Watanabe, T. Shibutani, N. Hirano, and S. Nakao